

Synthesis and electrochemical properties of cation doped spinel $\text{LiM}_{0.5}\text{Mn}_{1.5}\text{O}_4$ (M = Mn, Ni, and Al) cathode materials for Li-ion battery

Mesfin Kebede, Kenneth Ozoemena and Mkhulu Mathe

Energy Materials, Materials Science and Manufacturing, Council for Scientific and Industrial Research, P.O. Box 395, Pretoria, 0001, South Africa

E-mail: mkebede@csir.co.za

Abstract. Pristine LiMn_2O_4 and cation-substituted $\text{LiM}_{0.5}\text{Mn}_{1.5}\text{O}_4$ (M = Ni, Al) spinel cathode materials for lithium ion battery were synthesized using the solution-combustion of corresponding metal nitrate-urea solution mixtures. The particle size, morphology, structural and electrochemical properties of the as-synthesized powders were examined by means of scanning electron microscopy, X-ray diffraction, energy dispersive X-ray spectroscopy, charge/discharge battery testing. The effect of cation-doping on the discharge capacity retention was studied for different samples. Charge/discharge cycling studies show that both Ni and Al-substitution improves substantially the capacity retention of the spinel LiMn_2O_4 . It was found that both $\text{LiNi}_{0.5}\text{Mn}_{1.5}\text{O}_4$ and $\text{LiAl}_{0.5}\text{Mn}_{1.5}\text{O}_4$ compositions retain 99.8% of their respective first cycle discharge capacity of 102 mAh/g and 75 mAh/g, whereas LiMn_2O_4 retains only 60% of its first cycle discharge capacity of 122 mAh/g after 50 cycles.

1. Introduction

Recently, the development of cathode materials for lithium batteries that provide high voltage and cyclability becomes so significant to meet the demands for high-power applications such as hybrid electric vehicles and power tools. LiMn_2O_4 spinel as one of the most promising positive (cathode) materials attracted the interest of researchers, due to its low cost, environmental friendliness and good safety [1-2]. However, the problem with spinel LiMn_2O_4 cathode material is it suffers severe capacity loss upon repeated charge/discharge cycling at elevated temperature. Some of the causes for capacity fading might be related with Mn dissolution in acidic electrolytes [3], Jahn-Teller distortion of Mn^{3+} at deeply discharge state [4], and oxygen deficiency [5]. In order to tackle this problem, several research groups have synthesized cation substituted spinel materials $\text{LiM}_x\text{Mn}_{2-x}\text{O}_4$ such as (M= Ni, Al, Fe, Co) with an intension of getting high-voltage plateaus as well as enhancing the cyclability. Interestingly, the compound $\text{LiNi}_{0.5}\text{Mn}_{1.5}\text{O}_4$ with a cubic spinel structure has been characterized as a high-voltage around 4.9V cathode material for lithium ion batteries [6-7]. Similarly $\text{LiAl}_{0.5}\text{Mn}_{1.5}\text{O}_4$ spinel cathode material is reported as material with high voltage and cyclability [8].

Homogeneous dispersion of the cation substituting element in crystal lattice is so crucial in the synthesis of doped $\text{LiM}_{0.5}\text{Mn}_{1.5}\text{O}_4$ (M=Ni, Al) cathode materials. Generally solution synthesis techniques are preferable in order to get the required homogeneously doped composition without impurity unlike solid state reaction. Several solution synthesis methods of cation doped LiMn_2O_4 spinel structure have been reported, such as molten salt method [9], sol-gel method [10], pechini

process [11], hydrothermal [12], emulsion-drying method [13] have been used to establish the required physical and electrochemical properties of cathode material for rechargeable lithium-ion batteries. In this paper, we have followed a simple and time efficient solution technique to synthesize pristine LiMn_2O_4 and cation doped spinel structure $\text{LiM}_{0.5}\text{Mn}_{1.5}\text{O}_4$ ($\text{M}=\text{Ni}, \text{Al}$) cathode materials by combustion method using urea as reducer and fuel. In addition we have studied the effect of cation ($\text{Ni}^{2+}, \text{Al}^{3+}$) doping on the structural and the discharge capacity stability of the spinel LiMn_2O_4 cathode material.

2. Experiment

The pristine LiMn_2O_4 and cation-substituted oxide spinels $\text{LiM}_{0.5}\text{Mn}_{1.5}\text{O}_4$ ($\text{M}=\text{Ni}, \text{Al}$) were synthesized by the solution combustion method wherein stoichiometric amounts of the precursors 99.9% pure $\text{Li}(\text{NO}_3)$, $\text{Mn}(\text{NO}_3)_2 \cdot 4\text{H}_2\text{O}$, $\text{Ni}(\text{NO}_3)_2 \cdot 4\text{H}_2\text{O}$, $\text{Al}(\text{NO}_3)_3 \cdot 9\text{H}_2\text{O}$ and $\text{CH}_4\text{N}_2\text{O}$ were used. The procedure used to prepare LiMn_2O_4 and $\text{LiM}_{0.5}\text{Mn}_{1.5}\text{O}_4$ ($\text{M}=\text{Al}, \text{Ni}$) had the following stages. Appropriate mole ratios of Li, Mn, Ni and Al nitrate salts and urea were dissolved and mixed in deionised water with the various corresponding nitrate of the substituted cation(s). The precursor metal nitrates and urea were dissolved into deionised water and stirred at ambient temperature for about 30 min to obtain homogeneously mixed solution. After that, the precursor solution was introduced into a furnace preheated at 500°C and then black powders were obtained. To investigate the effect of Ni ion and Al ion on the structural and electrochemical properties of LiMn_2O_4 cathode materials, pristine LiMn_2O_4 and doped samples with Ni and Al ion concentration of 0.5 were prepared under atmospheric pressure and then annealed at 700°C in air for 10hrs. The voluminous and foamy combustion ash was easily milled to obtain the final LiMn_2O_4 and $\text{LiM}_{0.5}\text{Mn}_{1.5}\text{O}_4$ ($\text{M}=\text{Ni}, \text{Al}$) cathode materials. The annealed samples were subjected to different morphological SEM, elemental EDS, structural XRD, and electrochemical charge/discharge cycling characterization.

Coin cells of 2016 configuration were assembled using lithium metal as anode, Celgard 2400 as separator, 1M solution of LiPF_6 in 50:50 (v/v) mixture of ethylene carbonate (EC) and diethylene carbonate (DEC) as the electrolyte. The cathode was made through a slurry coating procedure from a mix containing active material powder, conducting black and poly(vinylidene fluoride) binder in N-methyl-2-pyrrolidone in the proportion 80:10:10, respectively. The slurry was coated over aluminium foil and dried at 120°C for 10h. 18mm diameter slurry-coated aluminium foils electrodes were punched out and used as cathode. Coin cells were assembled in an argon filled glove box (MBraun, Germany) with moisture and oxygen levels maintained at less than 1 ppm. The cells were cycled at 0.2C discharge rates in an MTI battery testing unit. The cells were cycled at 0.2C rate with respect to corresponding theoretical capacities of LiMn_2O_4 , $\text{LiNi}_{0.5}\text{Mn}_{1.5}\text{O}_4$ and $\text{LiAl}_{0.5}\text{Mn}_{1.5}\text{O}_4$ spinel and 30°C between 2.6 V and 4.9 V in a multi-channel battery tester.

3. Results and discussion

Fig. 1(a), (b), and (c) shows scanning electron microscope (SEM) image of LiMn_2O_4 , $\text{LiNi}_{0.5}\text{Mn}_{1.5}\text{O}_4$ and $\text{LiAl}_{0.5}\text{Mn}_{1.5}\text{O}_4$ samples, respectively. We can clearly see the voids on the morphology of materials in Fig. 1(c) caused by escaping gases during combustion synthesis. It is observed that the presence of Ni ion and Al ion has significance change on the morphology of powders. For a quantitative investigation on the particle size of the synthesized powders, we have plotted the particle size distributions of the powders in Fig. 2. Fig. 2a-c reveal that the particle size of synthesized structures LiMn_2O_4 , $\text{LiNi}_{0.5}\text{Mn}_{1.5}\text{O}_4$, and $\text{LiAl}_{0.5}\text{Mn}_{1.5}\text{O}_4$ are in the range of $0.9\ \mu\text{m}$ – $3\ \mu\text{m}$, 1.5 – $3.0\ \mu\text{m}$, and 0.45 – $0.9\ \mu\text{m}$, respectively. The pristine LiMn_2O_4 sample has a wider particle size distribution ranging from nanosize to microsize particles and do not exhibit Gaussian distribution, whereas doping of Mn ions by Ni^{2+} ion and Al^{3+} ion narrowed the particle size range and shows Gaussian distribution.

The particle size range for $\text{LiNi}_{0.5}\text{Mn}_{1.5}\text{O}_4$ samples is in microsize but for that of $\text{LiAl}_{0.5}\text{Mn}_{1.5}\text{O}_4$ is in nanosize. In addition, we have calculated the average particle size of the doped samples using the

Gaussian particle size distributions shown in Fig. 2. The average particle size of $\text{LiNi}_{0.5}\text{Mn}_{1.5}\text{O}_4$ and $\text{LiAl}_{0.5}\text{Mn}_{1.5}\text{O}_4$ samples are approximately $1.71\mu\text{m}$ and $0.6\mu\text{m}$, respectively.

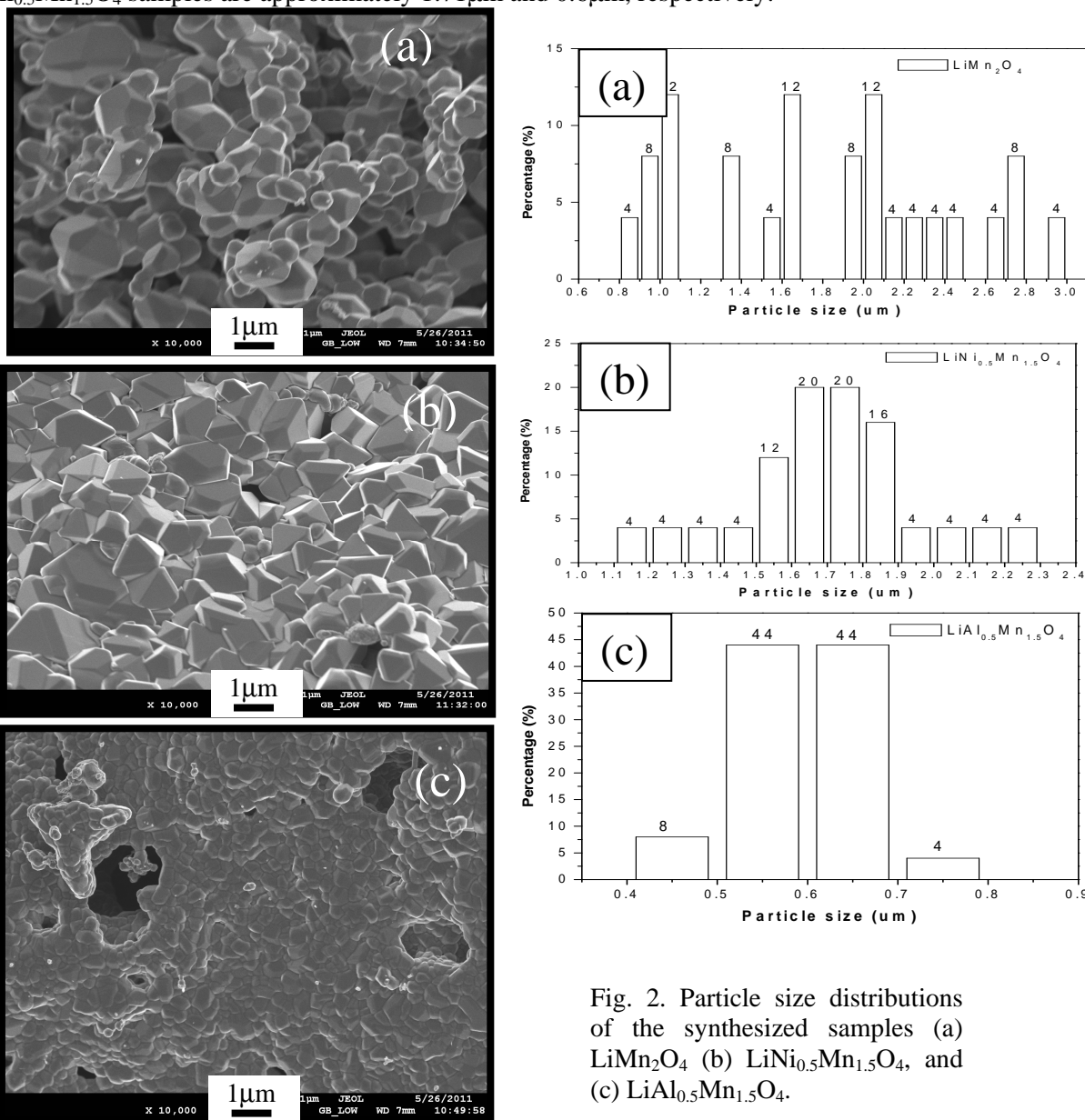


Fig. 2. Particle size distributions of the synthesized samples (a) LiMn_2O_4 (b) $\text{LiNi}_{0.5}\text{Mn}_{1.5}\text{O}_4$, and (c) $\text{LiAl}_{0.5}\text{Mn}_{1.5}\text{O}_4$.

Fig.1. (a), (b) and (c) are SEM images of pristine LiMn_2O_4 , $\text{LiNi}_{0.5}\text{Mn}_{1.5}\text{O}_4$ and $\text{LiAl}_{0.5}\text{Mn}_{1.5}\text{O}_4$, respectively

Energy dispersive X-ray spectroscopy (EDS) elemental analysis was carried out in order to confirm successful doping of cations. Though EDS cannot identify Li ion because of its small atomic size, it helped us to evaluate the cation doping in the samples. Fig.3 displays the EDS elemental spectra of the samples. The EDS spectrum confirms that the spinel LiMn_2O_4 cathode materials were successfully doped with Ni and Al ions using solution combustion techniques.

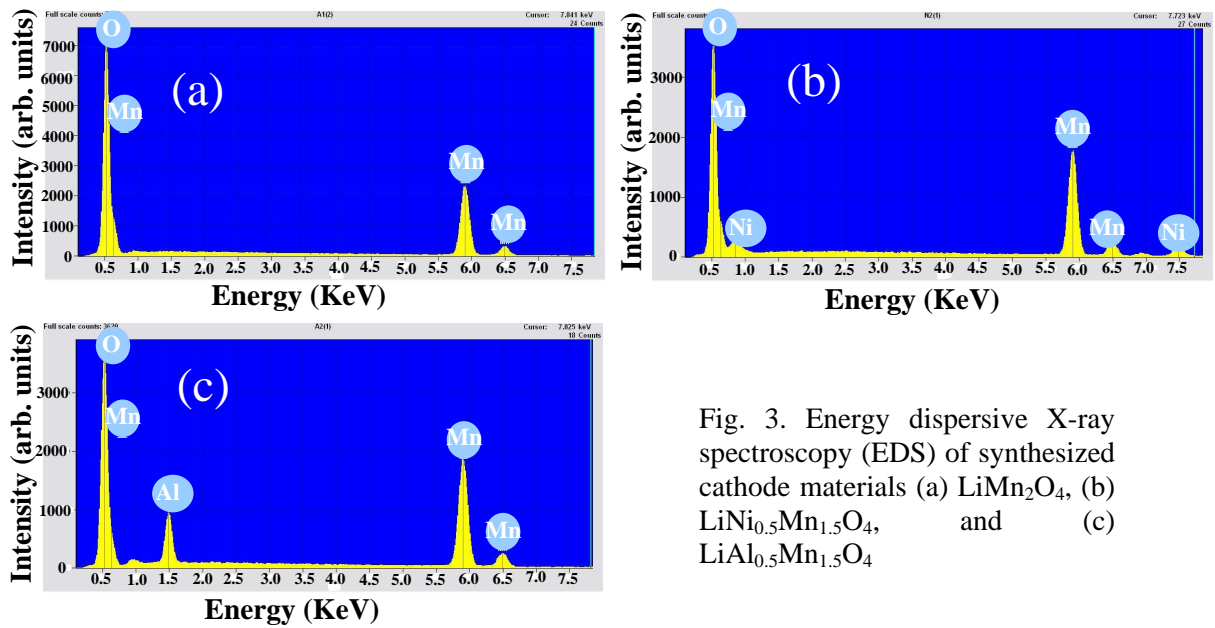


Fig. 3. Energy dispersive X-ray spectroscopy (EDS) of synthesized cathode materials (a) LiMn_2O_4 , (b) $\text{LiNi}_{0.5}\text{Mn}_{1.5}\text{O}_4$, and (c) $\text{LiAl}_{0.5}\text{Mn}_{1.5}\text{O}_4$

Fig. 4 shows a typical X-ray diffraction pattern of as-synthesized samples. The examination of the diffraction patterns confirms that all recognizable reflection peaks including (111), (311), (222), (400), (331), (511) and (440) can be clearly indexed to the single phase of the spinel cubic structure of LiMn_2O_4 (JCPDS File No. 88-1749) with space group $\text{Fd}\bar{3}\text{m}$ and with out any impurity peaks. All the peaks are very sharp, indicating a high crystallinity of the powders. The diffraction peaks systematically shift to higher angles and the lattice parameter decreases with the substitution of Ni^{2+} , or Al^{3+} for Mn^{3+} . Close investigation reveals that the crystal structure is shrunken with Ni^{2+} and Al^{3+} content in the doped LiMn_2O_4 phase.

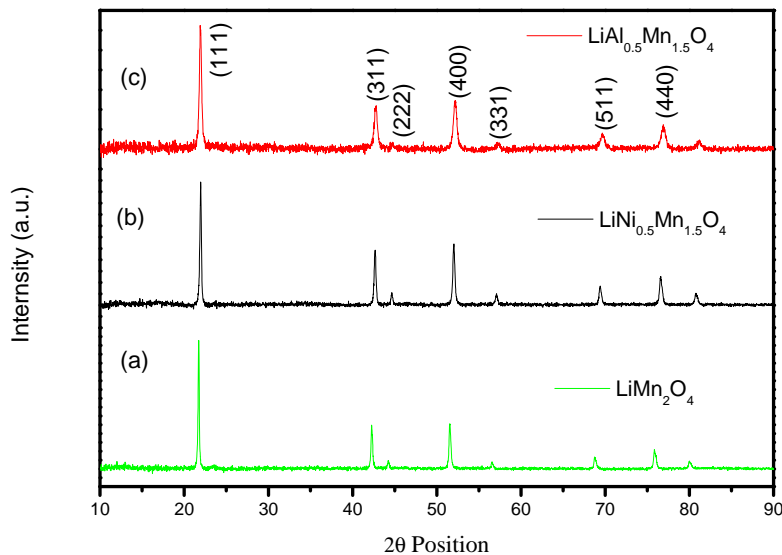


Fig. 4. X-ray diffraction pattern of synthesized (a) LiMn_2O_4 , (b) $\text{LiNi}_{0.5}\text{Mn}_{1.5}\text{O}_4$ and (c) $\text{LiAl}_{0.5}\text{Mn}_{1.5}\text{O}_4$ spinel cathode materials

It is generally believed that the lattice parameter in the cubic spinel structure depends on the Mn valence state. Thus, a small amount of Ni and Al increases the structural stability by the increase of mean Mn valence but the critical concentration of the dopant cation could hinder Li movement by occupation of the Li site.

The theoretical capacity, C_T , was calculated employing the well known expression:

$$C_T = 26.8 \frac{p}{M}$$

where p and M denote the number of Mn(III) and the molecular weight of ion-doped LiMn_2O_4 , respectively. Employing the above equation, the theoretical capacity of LiMn_2O_4 is found to be 148mAh/g, $\text{LiNi}_{0.5}\text{Mn}_{1.5}\text{O}_4$ is 146mAh/g and $\text{LiAl}_{0.5}\text{Mn}_{1.5}\text{O}_4$ is 80.3mAh/g, respectively. Charge/discharge capacity performance of the cathode materials carried out at 0.2C rates with respect to their corresponding theoretical capacities.

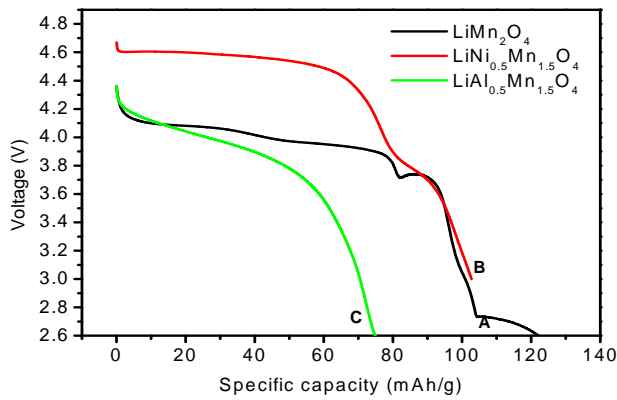


Fig. 5. First cycle discharge capacity of $\text{LiM}_{0.5}\text{Mn}_{1.5}\text{O}_4$ samples curve **A**, **B** and **C** for $M=\text{Mn}$, Ni and Al , respectively.

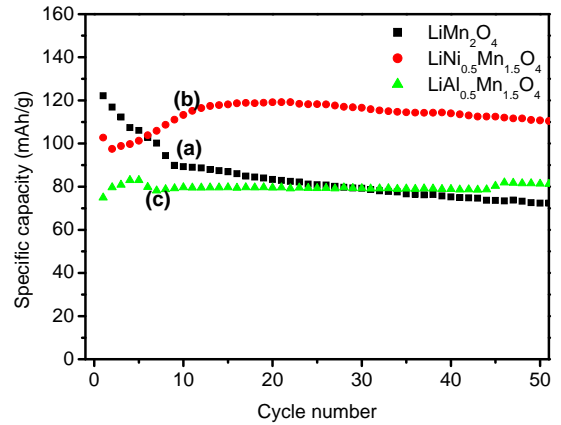


Fig. 6 The discharge capacity vs. cycle number for $\text{LiM}_{0.5}\text{Mn}_{1.5}\text{O}_4$ samples (a) $M=\text{Mn}$, (b) $M=\text{Ni}$ and (c) $M=\text{Al}$

The representative first cycle discharge capacities of LiMn_2O_4 , $\text{LiNi}_{0.5}\text{Mn}_{1.5}\text{O}_4$ and $\text{LiAl}_{0.5}\text{Mn}_{1.5}\text{O}_4$ are displayed by the curves **A**, **B**, and **C** in Fig. 5, respectively. During the first cycle pristine spinel LiMn_2O_4 delivered discharge capacity of around 122 mAh/g and plateau at 3.8V. As it can be seen in curve **B**, $\text{LiNi}_{0.5}\text{Mn}_{1.5}\text{O}_4$ gives discharge capacity of 102 mAh/g and exhibiting two plateau at around 4.6V and 3.8V due to the $\text{Ni}^{2+}/\text{Ni}^{4+}$ redox and $\text{Mn}^{3+}/\text{Mn}^{4+}$ redox couple, respectively [14]. Curve **C** depicts that $\text{LiAl}_{0.5}\text{Mn}_{1.5}\text{O}_4$ delivers discharge capacity of about 75 mAh/g which is comparable to experimentally reported values and close to the theoretical values. All the cathode samples prepared are well performing materials. It is noteworthy that the cell potential increases from 3.8V of LiMn_2O_4 to 4.6V for $\text{LiNi}_{0.5}\text{Mn}_{1.5}\text{O}_4$ and 4.0V for $\text{LiAl}_{0.5}\text{Mn}_{1.5}\text{O}_4$ and the doped materials can be considered as high voltage cathode materials.

To compare and examine the battery performance of as-synthesized pristine and cation doped cathode materials, 50 charge/discharge cycles of a lithium battery employing LiMn_2O_4 , $\text{LiNi}_{0.5}\text{Mn}_{1.5}\text{O}_4$ and $\text{LiAl}_{0.5}\text{Mn}_{1.5}\text{O}_4$ cathode were performed between 3.0 and 4.9 V at a constant current of 0.2C rate. Fig. 6 curve (a) is obtained from the pristine LiMn_2O_4 and it retained only 60% of its first cycle capacity of 122mAh/g. Fig. 6 curve (b) and curve (c) respectively represents cyclic performance of $\text{LiNi}_{0.5}\text{Mn}_{1.5}\text{O}_4$ and $\text{LiAl}_{0.5}\text{Mn}_{1.5}\text{O}_4$. Both cation substituted samples $\text{LiNi}_{0.5}\text{Mn}_{1.5}\text{O}_4$ and $\text{LiAl}_{0.5}\text{Mn}_{1.5}\text{O}_4$

exhibited a very good cyclability, they retained 99.8% of their respective first cycle after 50 cycles, however the first cycle capacity of $\text{LiAl}_{0.5}\text{Mn}_{1.5}\text{O}_4$ is low compared with $\text{LiNi}_{0.5}\text{Mn}_{1.5}\text{O}_4$. The capacity retention of the Ni and Al-substituted spinels is significantly enhanced in comparison with that of LiMn_2O_4 . The possible reasons for the observed behaviour are, first there may be a considerable decrease in the effect of Jahn-Teller distortion when substituting a small amount of Ni and Al for Mn in the spinel. Second, there may be a reduction in spinel dissolution.

4. Conclusion

In summary, we concluded that pristine LiMn_2O_4 and cation doped $\text{LiM}_{0.5}\text{Mn}_{1.5}\text{O}_4$ (M=Ni, Al) oxide prepared by the solution combustion method can be applied for Li-ion batteries cathode material. The samples were characterized by SEM, EDS, XRD, and battery charge/discharge testing. The particle size distribution affected by the kind of the doping ion, Ni ion exhibited big particle size but Al ion exhibit small particle size. Both cation substitute samples showed high cyclability of 99.8%. In addition, we have found that the sample $\text{LiNi}_{0.5}\text{Mn}_{1.5}\text{O}_4$ exhibited higher first cycle discharge capacity and high working voltage than $\text{LiAl}_{0.5}\text{Mn}_{1.5}\text{O}_4$ sample. The variation in lattice parameter as a result of Ni and Al doping greatly enhanced the cyclability of discharge capacity of the LiMn_2O_4 spinel.

Acknowledgments

We thank CSIR for supporting this work. MK thanks NRF for supporting this work financially.

References

- [1] T. Ohzuku, M. Kitagawa and T. Hirai, *J. Electrochem. Soc.*, 137 (1990) 769.
- [2] R. J. Gummow, A. Dekock, M. M. Thackeray, *Solid State Ionics* 69 (1994) 59–67
- [3] D.H. Jang, Y.J. Shin, S.M. Oh, *J. Electrochemical Society* 143 (1996) 2204-2211
- [4] T. Ohzuku, M. Kitagawa, T Hirai, *J. Electrochemical Society* 137 (1990) 769-775
- [5] Y.Y. Xia, T. Sakai, T. Fujieda, X.Q. Yang, Z.F. Ma, J. McBreen and M. Yoshio, *J. Electrochem. Soc.*, 148 (2001) A723
- [6] K. Amine, H. Tukamoto, H. Yasuda, Y. Fujita, *J. Power Sources*, 68 (1997) 604
- [7] R. Alcántara, M. Jaraba, P. Lavela, J. L. Tirado, *Electrochimica Acta*, 47(2002)1829
- [8] R. Thirunakaran, A. Sivashanmugam, S. Gopukumar, Charles W. Dunnill, Duncan H. Gregory, *J. Mater. Processing technology* 208 (2008) 520-531
- [9] Yang, X.; Tang, W.; Kanoh, H.; Ooi, K. *J. Mater. Chem.*, 9 (1999) 2683
- [10] S. Bach, M. Henry, N. Baffier, J. J. Livage, *Solid State Chem.* 88 (1990) 325–333
- [11] M. S. Whittingam, *Solid State Ionics* 86-88 (1996) 1-7
- [12] S.-H. Wu, H.-L. Chen, *J. Power Sources* 119-121 (2003) 134
- [13] K.-T. Hwang, W.-S. Um, H.-S. Lee, J.-K. Song, K.-W. Chung, *J. Power Sources* 74 (1998) 169
- [14] Y. J. Lee, C. Eng, C. P. Grey, *J. Electrochem. Soc.*, **148** (2001) A249